Journal of Environmental Chemical Engineering 9 (2021) 104760

Contents lists available at ScienceDirect

Journal of Environmental Chemical Engineering

journal homepage: www.elsevier.com/locate/jece

Optimization the removal of lead ions by fungi: Explanation of the mycosorption mechanism

Zeynep Mine Şenol [a], Ülküye Dudu Gül [b,*], Rafig Gurbanov [c], Selçuk Şimşek [d]

[a] Cumhuriyet University, Zara Vocational School, Department of Food Technology, 58140, Sivas, Turkey
[b] Bilecik Seyh Edebali University, Vocational School of Health Services, Biotechnology Application and Research Center, 11230, Bilecik, Turkey
[c] Bilecik Seyh Edebali University, Department of Molecular Biology and Genetics, Biotechnology Application and Research Center, 11230, Bilecik, Turkey
[d] Cumhuriyet University, Faculty of Science, Department of Chemistry, 58140, Sivas, Turkey

ARTICLE INFO

Editor: Teik Thye Lim

Keywords:
Attenuated total reflectance-fourier transform infrared spectroscopy
Lead removal
Mycosorption
Rhizopus arrhizus

ABSTRACT

The potential utilization of fungal biomass (*Rhizopus arrhizus*) as a biosorbent for the efficient removal of lead (Pb^{2+}) ions from aqueous solutions was optimized in the current work. The maximum Pb^{2+} biosorption capacity of fungal biosorbent was 0.501 mol kg^{-1} at pH 4.0 and 25 °C. The biosorption process follows the intra-particle diffusion and pseudo-second-order rate kinetics. Thermodynamic studies showed that Pb^{2+} biosorption by this fungal biosorbent is spontaneous and endothermic. The fungus has good biosorption/desorption performance for Pb^{2+} ions according to desorption studies. The biosorption free energy calculated from the Dubinin-Radushkevich isotherm showed that the biosorption process was accomplished chemically. Moreover, the mechanism of the Pb^{2+} biosorption on to the fungal biosorbent was evaluated by infrared spectral analysis coupled with pattern recognition techniques using Attenuated Total Reflectance-Fourier Transform Infrared Spectroscopy (ATR-FTIR). The ATR-FTIR spectral analysis of the fungal biosorbent revealed changes in particular spectral bands emerging from functional groups of biomolecules. Possibly, these functional groups of biomolecules are active fungal biosorbent sites involved in the interaction with Pb^{2+} ions. Thus, the surface of the fungal biosorbent is attractive for the sorption of metal ions making the fungal biomass as an effective and efficient biosorbent for the removal of Pb^{2+} ions.

1. Introduction

The industrial development resulted in an increase in the heavy metal contamination in the environment due to their metal containing effluents. The wastewater of metal plating, mining, battery, and paper industries contains a large number of heavy metals [1,2]. The industrial wastewater containing heavy metals is discharged into the water resources and these toxic heavy metals are accumulated by the living organisms. For example, lead caused health problems in the nervous and reproductive system of humans [3]. Heavy metals are the most priority pollutants in the environment as they cannot biodegraded naturally. Therefore, it is very important to remove high concentrations of these pollutants from the water resources. Accordingly, new technologies are suggested for the decontamination of heavy metal-containing wastewater [4]. However, the vast majority of these methods are time-consuming, expensive, and non-eco-friendly [5].

Among wastewater treatment methods, biological ones are suggested as low-cost and environment-friendly [6]. Biosorption is a term that results from the use of biological or biological originated materials as an adsorbent in the adsorption method and the adsorbents used in biosorption are called biosorbent. Effective interactions occur between the biosorbent and adsorbate in biosorption, just like in adsorption, and these interactions occur physically or chemically during the adsorption process. The characterization of these chemical and physical interactions is also important to explain the biosorption mechanisms.

Fungal biomass is commonly used as a biosorbent in biological wastewater treatment [7]. Recent studies defined fungal biosorption as mycosorption [8]. Cell wall structures play an important role in the functioning of fungi as successful biosorbents [9]. The interaction of the components that make up the cell wall structure with the pollutants such as dyes and heavy metals in aqueous environments is the main element of the biosorption mechanism.

In general, it is known that the fungal cell wall contains glucans, mannoproteins, and chitin in the chemical composition [10]. The

* Corresponding author.
E-mail address: ulkuyedudu.gul@bilecik.edu.tr (Ü.D. Gül).

https://doi.org/10.1016/j.jece.2020.104760
Received 25 August 2020; Received in revised form 1 November 2020; Accepted 7 November 2020
Available online 11 November 2020

glucans provide the strength of the cell wall and these are shaped in microfibrillar structure. The major component in the wall structure is β - glucan and these β glucans are available as β 1,3 glucan or β 1,6 glucan or both [11]. The cell wall layer is in the form of β 1,3 glucans and chitin. Chitin is a polymer of N-acetylglucosamine and forms up to the second majority component of the fungal cell walls [12, 13]. In the fungal cell wall structure, the chitin is believed to occur in the form of linear chains. Cell wall proteins are bound to the β 1,3 glucan - chitin network either indirectly with a β 1,6 glucan moiety or directly by covalent bonds. The mechanical strength and durability of the cell wall depend on the β 1,3 glucans present in its structures. β 1,3 glucan is included in the so-called hollow helix family. In other words, β 1,3 glucan chains resemble a flexible spring wire that can expand. This feature explains the elasticity of the cell wall. Mannoproteins are attached to the outer surface of the β 1,3 glucan - chitin layer and 90 % of these proteins are glycosylated by carbohydrate fractions. Mannoproteins are important in cell permeability, but they can act as structural proteins by acting as agglutinins. The mannoprotein layer that forms the outer layer is less permeable than the fibrillar layer inside. The low permeability property occurs due to asparagine roots and the presence of disulfide bridges, highly branched, and long carbohydrate side chains. The fungal cell surface contains a large number of negative charges, due to the phosphodiester bridges in the N- and O- linked mannose side chains [8,14]. Polysaccharides play a central role in cell wall organization. In possible synthesis mechanisms, proteins are attached to polysaccharides in the cell wall, and bonds of physiological importance are established [15]. There are two main classes of proteins that are covalently linked to cell wall polysaccharides and are GPI-dependent cell wall proteins and Pir proteins (Pir-CWPs). GPI - dependent cell wall proteins are proteins that indirectly bind to 1,3 glucans. These proteins are first bound to 1,6 glucan and then to 1,3 glucans. They also need GPI for this attachment. Pir proteins can be directly attached to 1,3 glucans. Cell wall proteins have various functions such as cell wall permeability, water retention, and adhesion. They are also cell wall proteins that coordinate metabolism events such as the uptake of various metals such as iron into the cell [11]. It is also thought that these proteins can interact with various heavy metals that are used as adsorbate and cause water pollution and thus may play a role in the biosorption mechanism.

From past to present fungal biosorbents have been investigated to remove heavy metal ions. Especially in recent studies, it is pointed out that chitin or chitosan (an important component of the fungal cell wall) based adsorbents are successful agents in removing cations such as heavy metals [16]. Previously, many biosorption studies have been performed with fungal biomass, especially the biomass of fungi belonging to the *Rhizopus* genus [17–21]. The results of these studies showed that the biomass of *Rhizopus* genera was a successful candidate for mycosorption of heavy metals. However, the mechanism involved in the realization of mycosorption by the fungus has not been explained in these previous studies. This study aims to optimize the potential of fungal biosorbent obtained from *Rhizopus arrhizus* for lead biosorption and to explain the biosorption mechanism. In the explanation of the biosorption mechanism, Attenuated Total Reflectance-Fourier Transform Infrared (ATR-FTIR) Spectroscopy coupled with pattern recognition methods were utilized due to the accuracy, versatility, and high analytical capacity of this fingerprinting technique [22]. To the best of our present knowledge, this is the first study reporting ATR-FTIR spectroscopic analyses to explain the molecular interactions happening during the fungal biosorption process in terms of lead removal. ATR-FTIR spectroscopy is a high-throughput vibrational spectroscopic technique in the identification of molecule-specific spectral bands and provides direct molecular information about the biochemical composition of any biological material including bacteria and fungi [23]. Since the FTIR spectra contain complex biochemical information, pattern recognition methods are necessary for the proper analysis and interpretation of data. These data mining approaches simplify the complexity of big data, in which meaningful information can be gathered rapidly and systematically [24]. Taking all together, infrared spectroscopy coupled with pattern recognition methods is important to track diverse biological processes in both scientific studies and the biotech industry. Therefore, it is expected that the findings presented herein will contribute to the mycosorption literature. Furthermore, the fungal biosorbent was cultivated in a medium composed of molasses, which is a secondary waste of sugar refinery to obtain inexpensive biosorbent material and thereby reduce the cost of the lead-biosorption process.

2. Materials and methods

2.1. Preparation of biosorbent

The fungal strain (*Rhizopus arrhizus)* was provided by the US Department of Agriculture Culture Collection. The preparation of a molasses medium was previously given in [6]. The molasses, obtained for free from the sugar refinery factory manufacturing sugarcane, and used as a low-cost carbon source for fungal growth [6]. Miljkovic et al. 2016 stated that molasses obtained from sugarcane was an inexpensive carbon source having rich sucrose ingredients for the preparation of medium [25]. Similarly, Xie et al. 2017 emphasized that they preferred sugarcane molasses to reduce the cost of fungal cultivation as a rich nutritional source [26]. In addition to this, Gül (2013) showed that molasses was a promising alternative carbon source for the growth of *R. arrhizus* [6]. Thus, the freely-available sugar factory waste molasses as a low-cost alternative method was used in this study to obtain fungal biomass. The fungus was inoculated into a molasses medium at pH 4.5 and 30 °C which were optimal conditions for fungal cultivation [6]. After ten days of the incubation period, the biomass of the fungus was harvested, washed, and treated with distilled water and a 1% formaldehyde solution, respectively. Then the biomass dried at 60 °C for 24 h and smashed for usage in experiments, respectively.

2.2. Chemicals

$Pb(NO_3)_2$ in the adsorption study of Pb^{2+} ion, 4- (2-pyridyl azo) resorcinol (PAR), and other chemicals were achieved from Merck (Germany). All experiments were studied in duplicate. Ultrapure water was used in all experiments.

2.3. Methods of analysis

The concentration of Pb^{2+} ions was determined by measuring the UV–vis spectrophotometric method of the complex formed by PAR [27]. PAR was used as a complex-forming reagent for the determination of Pb^{2+} in the supernatants. A solution of 3.5×10^{-3} mol L^{-1} of PAR in 0.7 mol L^{-1} of Tris/HCl at pH 8.0–9.0 was prepared. A 50 μL fraction of supernatant was added onto 3 mL of the reagent and the absorbance of the formed metal complex was measured at λ =518.5 nm for Pb^{2+}.

2.4. Characterization techniques

2.4.1. SEM-EDX analysis

Scanning Electron Microscopy (SEM) with Energy Dispersive X-Ray Analysis (EDX) is commonly used for characterization of biosorbent before and after the biosorption process. The surfaces of unloaded and Pb^{2+} loaded fungal biosorbent were characterized by SEM-EDX analyses. SEM images and EDX compositional data of unloaded and Pb^{2+} loaded fungal biosorbent were obtained with a Leo 440 Computer Controlled Digital System. The dried fungal biomass was prepared for the SEM-EDX analysis [28] after treatment with the operational conditions (V = 10 mL) of 300 mg L^{-1} Pb^{2+} ion concentration with 30 mg biosorbent dosage at pH 4.0 and 25 °C.

2.4.2. Infrared spectral analysis

FTIR spectrometer (Frontier FTIR with ATR Miracle attachment/

PerkinElmer, US) was used for sampling the spectra of unloaded (UL group) and Pb^{2+} loaded (PL group) fungal biomasses. The reference spectrum was obtained by sampling air at room temperature. The powdered and dried samples were positioned on a Zn-Se crystal of ATR accessory in equivalent amounts. The experiment was conducted in the 4000−650 cm^{-1} spectral interval with 64 scan numbers at 4 cm^{-1} resolution [23].

2.4.3. Pattern recognition technique: Principal component analysis

Principal component analysis (PCA) was applied to the mean-centered raw absorbance spectra in the fingerprint (1800−650 cm^{-1}) and C–H (3000−2800 cm^{-1}) regions via The Unscrambler X 10.4 (Camo, NO) software. Full Cross Validation method, Singular Value Decomposition (SVD) algorithm, and Hotelling's T2 statistics were used in the model, and results were presented as scores and loadings plots.

2.4.4. Pattern recognition technique: Hierarchical cluster analysis

Hierarchical cluster analysis (HCA) was applied to the raw absorbance spectra in the fingerprint (1800−650 cm^{-1}) and C–H (3000−2800 cm^{-1}) regions via The Unscrambler X 10.4 (Camo, NO) software. Ward's method using Squared Euclidean distance (1800−650 cm^{-1}) and Average linkage clustering using Chebyshev distance (3000−2800 cm^{-1}) was applied in the model. Clustering was based on either the magnitude of similarities or distance between the spectra and the result was presented as a dendrogram.

2.4.5. Point of zero charges for Rhizopus arrhizus

The solution pH at which the surface charge of the biosorbent becomes zero is defined as the point of zero charges (PZC). To determine the PZC values of the *Rhizopus arrhizus*, 0.1 mol L^{-1} KNO_3 solutions were prepared and their initial pHs were adjusted in the range of 1.0–12.0 by NaOH and HCl. Then 10 mL of KNO_3 and 100 mg biosorbent was incubated for 24 h in pH solutions ranging from 2.0- to 12.0. The samples were kept at 25 °C for 24 h and the final pHs of solutions were measured by using a pH meter (Selecta, Spain). The graph was plotted using initial versus final pHs, and the PZC was determined by the obtained experimental results.

2.5. Biosorption experiments

Biosorption experiments were investigated by using the batch method. Stock Pb^{2+} solution (1000 mg L^{-1}) was prepared using double distilled water. For the adsorption experiments, 30 mg of fungal biosorbent was put into 10 mL of Pb^{2+} solution (300 mg L^{-1}). The adsorption was carried out at 25 °C and both fungal biosorbent and Pb^{2+} in polypropylene tubes of 10 mL were kept in a thermostatic water bath with constant agitation speed (140 rpm) for 24 h. The pH was adjusted with dilute HCl and NaOH solutions (each one, 0.1 and/or 1.0 mol L^{-1}). The influences of pH (1.0–5.0), biosorbent dosage (0.1–20 g L^{-1}), Pb^{2+} concentration (10–600 mg L^{-1}), time (2–1440 minutes), and temperature (5, 25, and 40 °C) on biosorption were examined at batch level experiments to determine optimal conditions for maximal biosorption performance. Desorption experiments were carried out at optimal conditions determined at biosorption assays. Pb^{2+} ion concentration was determined by the absorbance measurement. % Biosorption and Q (mol kg^{-1}) were calculated with Eqs. 1 and 2.

$$\%Biosorption = \left[\frac{C_i - C_f}{C_i}\right] x100 \tag{1}$$

$$Q = \left[\frac{C_i - C_f}{m}\right] xV \tag{2}$$

In these equations; C_f is the equilibrium concentration (mg L^{-1}), C_i is the initial concentration of the biosorbent (mg L^{-1}), m refers to the biosorbent mass (g), V is the solution volume (L) and Q is the adsorption capacity (mol kg^{-1}).

2.6. Desorption experiments

Desorption studies were performed for biosorbent recovery and reuse in biosorption processes. In this study, dilute 1 M HCl, 1 M NaOH, 1 M HNO_3, and 1 M Ethyl alcohol solutions (each one, 0.1 mol L^{-1}) were used for desorption of the Pb^{2+} ions from the surface of the fungal biosorbent. To determine the recovery property of the biosorbent, the experiments were repeated three times with the same biosorbent for the biosorbent/desorption cycle. At the end of each experiment, the solutions were centrifuged at 5000 rpm for 10 min to ensure liquid-solid separation and the amount of Pb^{2+} ions in the equilibrium solution was determined by UV–vis spectrophotometric method. % Desorption was calculated with Eq. 3.

$$Desorption\% = \frac{Q_{des}}{Q_{ads}} x100 \tag{3}$$

In this equation; Q_{des}; the amount of desorption capacity (mol kg^{-1}), Q_{ads}; the adsorbed amount of adsorption capacity (mol kg^{-1}).

2.7. The calculation of biosorption isotherms, kinetics, and thermodynamics

The adsorption of Pb^{2+} ions onto fungal biosorbent was modeled using the Langmuir, Freundlich, and Dubinin-Radushkevich (D–R) isotherm models. The Langmuir isotherm theory assumes that adsorption takes place at specific homogeneous sites within the adsorbent and that adsorption is a monolayer. The Freundlich isotherm theory assumes that adsorption occurs on heterogeneous surfaces. The D–R isotherm model examines adsorption energetically. The Langmuir, Freundlich, and D–R isotherm equations are expressed by the following Eqs. 4–6, respectively.

$$Q = \frac{X_L K_L C_e}{1 + K_L C_e} \tag{4}$$

$$Q = K_F C_e^{\beta} \tag{5}$$

$$Q_e = Q_{DR} e^{-K_{DR}\varepsilon^2} \tag{6}$$

where Q (mol kg^{-1}) is the amount of adsorption capacity, X_L (mol kg^{-1}) is the maximum adsorption capacity, K_L (L mol^{-1}) is the parameter for Langmuir isotherm and C_e is the equilibrium concentration (mol L^{-1}), and K_F: Freundlich constant, β: adsorbent surface heterogeneity. X_{DR} (mol kg^{-1}) is a measure of adsorption capacity, ε (mol^2 K J^2) is the Polanyi potential coefficient and K_{DR} (mol^2 K J^{-2}) is the activity, R is the ideal gas constant (8.314 J mol^{-1} K^{-1}) and T (K) is the absolute temperature. The Polanyi potential (ε) is expressed by the following Eq. 7.

$$\varepsilon = RTln\left(1 + \frac{1}{C_e}\right) \tag{7}$$

The adsorption energy (E) is expressed by the following Eq. 8.

$$E_{DR} = (2K_{DR})^{-0.5} \tag{8}$$

If the adsorption energy is 8 < E_{DR}<16 kJ mol^{-1}, the adsorption is chemically controlled and E_{DR}<8 kJ mol^{-1} indicates that the adsorption proceeds physically [22].

The kinetic study is very important in batch experiments to find the optimum interaction time of metal ions with biosorbent. The three most commonly kinetic models were used to evaluate the contact time dependence of the adsorption process. The adsorption kinetics of Pb^{2+} ions onto fungal biosorbent was described by pseudo-first-order (PFO), pseudo-second-order (PSO), and intraparticle diffusion (IPD) kinetic model equations are given as Eqs. 9–11, respectively [27].

$$Q_t = Q_e\left[1 - e^{-k_1 t}\right] \tag{9}$$

$$Q_t = \frac{t}{\left[\frac{1}{k_2 Q_e^2}\right] + \left[\frac{t}{Q_e}\right]} \quad (10)$$

$$Q_t = k_i t^{0.5} \quad (11)$$

where Q_t (mol kg^{-1}) is the adsorption capacity at time t (min), Q_e (mol kg^{-1}) is the adsorption capacity at equilibrium, k_1, k_2, and ki is the rate constant of the PFO (min^{-1}), the PSO model (mol^{-1} kg min^{-1}) and the intra IPD (mol^{-1} kg $min^{-0.5}$) model, respectively.

In this study, the mass transfer factor (MTF) models developed by Fulazzaky [28] was used to assess the biosorption behavior of Pb^{2+} ions onto fungal biosorbent accompanied aiming at a good understanding of the wide applicability of the models. Therefore, the use of the following equations [28,29] would be able to describe the biosorption kinetics of Pb^{2+} ions onto fungus biosorbent, such that;

$$ln\left(\frac{C_0}{C_s}\right) = [k_L a]_g x e^{-\beta x q} x t \quad (12)$$

$$q = \frac{1}{\beta} x ln(t) + B \quad (13)$$

$$B = \frac{ln([k_L a]) - ln\left\{ln\left(\frac{C_0}{C_s}\right)\right\}}{\beta} \quad (14)$$

where $[k_L a]_g$ is the global mass transfer factor (min^{-1}), β is the biosorbate-biosorbent affinity parameter (kg min mol^{-1}), and t is accumulation time (min). B and β are obtained from ln(t) against q the graph. The slope (β) and y-intercept (B) have been verified from a straight line of plotting q versus ln(t). And then a curve of plotting $[k_L a]_g$ versus C_s/C_0 can be proposed to get an insight on global mass transfer (GMT) for the biosorption of Pb^{2+} ions onto fungal biosorbent. The mathematical equation to express the relation of external to global mass transfer is as follows [28];

$$[k_L a]_f = [k_L a]_g e^{-\beta x q} \quad (15)$$

$[k_L a]_f$ is the external mass transfer factor or film mass transfer factor or volumetric film mass transfer coefficient (min^{-1}). And then a curve of plotting $[k_L a]_f$ versus C_s/C_0 can be proposed to get an insight on external mass transfer (EMT) for the biosorption of Pb^{2+} ions onto fungal biosorbent. The internal mass transfer (IMT) factor can be calculated with the following equation [28];

$$[k_L a]_d = [k_L a]_g - [k_L a]_f \quad (16)$$

where $[k_L a]_d$ is an internal mass transfer factor (min^{-1}). Using Eq. 16 permits us to compute the values for variable $[k_L a]_d$ following the C_s/C_0 ratio since the values for both variables $[k_L a]_g$ and $[k_L a]_f$ have been verified [28].

Thermodynamic parameters are necessary to explain whether the biosorption process is spontaneous or not. Enthalpy and entropy (ΔH° and ΔS°) are obtained from lnK_D against 1/T the graph. The slope (-ΔH°/R) and y-intercept (ΔS°/R) of the data plotted as lnK_D against 1/T the graph. The K_D is calculated from Eq. 17. ΔH°, ΔS°, and the Gibbs free energy (ΔG°) are calculated using the following equations (Eqs. 18–20, respectively);

$$K_D = \frac{Q}{C_e} \quad (17)$$

$$\Delta G = -RTlnK_D \quad (18)$$

$$lnK_D = \frac{\Delta S^0}{R} - \frac{\Delta H^0}{RT} \quad (19)$$

$$\Delta G^0 = \Delta H^0 - T\Delta S^0 \quad (20)$$

where R is the ideal gas constant (8.314 Jmol-1 K-1), T is the absolute temperature (K).

3. Results and discussion

3.1. Effect of pH on biosorption and point of zero charges (PZC)

Interactions between functional groups on the surface of the biosorbent and metal ions were known to be influenced by the pH of the medium. The pH of the solution medium is directly interested in the competitiveness of the metal ions with hydrogen ions to the active centers on the biosorbent surface. At highly acidic pHs, metal cations and hydrogen ions compete for binding to active sites, resulting in less biosorption of the metal. At high alkali pHs, soluble hydroxide complexes of metal ions are formed which reduces biosorption. The zeta potential is used to characterize the surface charge of the adsorbents [27] and the surface charge is affected by the solution pH in adsorption experiments. The pH_{pzc} is used to determine the zeta potential and the surface charge is negative at the pH values above the pH_{pzc} [27]. The pH_{pzc} value of the *R. arrhizus* was found 4.67 (Supplementary File 1) indicated that the surface charge of the fungus was negative at pH 4.

The results related to the effect of pH on the biosorption of Pb^{2+} ions by fungus are presented in Fig. 1. According to the results, the percentage of the biosorption rate increased from 17 % to 79 % with increasing pH value from 1 to 4, respectively. Similarly, Javanbakht et al. 2011 stated that increasing pH values up to around pH 5 caused higher Pb^{2+} biosorption by another fungal biosorbent called *Mucor indicus* [30]. It was reported that the biosorbent surface became deprotonated due to the increasing negatively charged groups on the biosorbent surface at higher pH values and tent to interact with metal cations, therefore the metal biosorption by the fungus was enhanced [31]. Manzoor et al. 2012 showed that the biosorbent obtained from *R. arrhizus* performed both Cu^{2+} and Ni^{2+} ions at higher pH values up to around 5 [32]. In the results of the current study, the maximum Pb^{2+} biosorption rate was found as 79 % at pH 4, which was the natural pH of 300 mg L^{-1} (1.5 × 10^{-3} M) Pb^{2+} solution. Therefore, all biosorption experiments were carried out at the natural pH of the Pb^{2+} ion. The pH of the solution at pH 5 and above were not studied due to the precipitation of Pb^{2+}ions as hydroxides.

3.2. The effect of biosorbent dosage

The effect of the biosorbent dosage on the biosorption of Pb^{2+} ions was studied in the range of 0.1−20 g L^{-1}. The results given in Supplementary File 2 showed that the biosorption yield increased with the amount of fungal biosorbent increased due to the increase in active sites

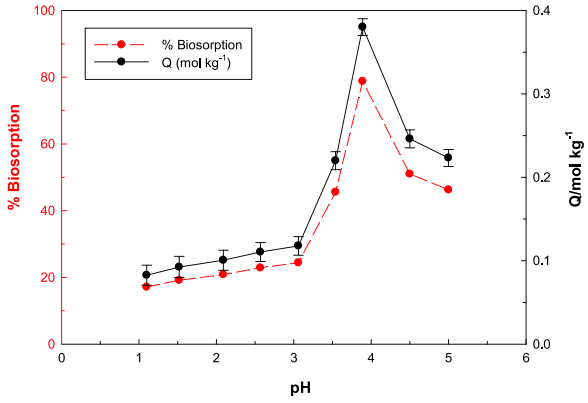

Fig. 1. The effect of pH on biosorption of Pb^{2+} by fungal biosorbent ($[Pb^{2+}]_0$ = 300 mg L^{-1}, biosorbent dosage = 30 mg, V = 10 mL, pH = 1.0-5.0, contact time:24 h, temperature: 25 °C).

on the biosorbent surface. Thus, metal ions penetrated more easily into the biosorption sites [31]. The maximum biosorption was found to be approximately 90 % in the amount of 20 g L^{-1} biosorbent. As the number of active sites for biosorption increases due to the increase in biosorbent dosage, the biosorption of Pb^{2+} ions onto the fungal biosorbent has increased with the increased amount of biosorbent. Similarly, Kiliç et al., 2014 reported that increasing biosorbent dosage caused an increment of biosorption rate due to the increased surface area for adsorption of metal ions [33].

3.3. Effects of initial Pb^{2+} concentration and contact time

The changes of % biosorption and Q (mol kg^{-1}) values with the initial Pb^{2+} concentration is given in Supplementary File 3. The number of adsorbed ions increased with increasing ion concentration and the percentage of biosorption was decreased. The initial concentration has an important effect in overcoming the mass transfer resistance formed between the ion in the solution and the solid surface. Supplementary File 3 shows that there is a higher % biosorption rate at low Pb^{2+} ion concentrations, and with the increase of initial Pb^{2+} ion concentration, active biosorption sites on the fungal biosorbent decreased over time and reached saturation. It was observed that % biosorption value has decreased from 98 % to 51 % at 25 and 600 mg L^{-1} Pb^{2+} ion concentrations, respectively. This reduction was due to an effective mass transfer between the initial Pb^{2+} ion concentration and the biosorbent surface.

3.4. Biosorption isotherms

The harmony to the Langmuir, Freundlich, and Dubinin-Radushkevich isotherm models was presented in Fig. 2. Table 1 shows the parameters used in the isotherms. The maximum biosorption capacity was calculated to be 0.501 mol kg^{-1} and the K_L value was 4976 L mol^{-1} from the Langmuir isotherm model. Pb^{2+} biosorption onto fungal biosorbent fitted well with the Langmuir model. The Freundlich isotherm model, K_f 4.87 is a measure of the biosorption capacity. β surface heterogeneity was found to be 0.340. The D–R isotherm model, EDR 12.4 kJ mol^{-1} is a measure of the biosorption energy. Freundlich parameter indicates the degree of heterogeneity of the surface, and the EDR value found in the D–R model indicates that the biosorption process is chemical.

In adsorption studies, the adsorption amounts and working concentrations of the solutions with the adsorbents of different initial concentrations allow isotherms to be compatible with widely used adsorption models, Langmuir, Freundlich, and DR models, and find adsorption parameters. The Langmuir model is a model used to define isotherms that exhibit hyperbola behavior, that is, reach equilibrium with the filling of the adsorption centers as the concentration increases and there is no change in the adsorption although the concentration increases. By investigating the compatibility of the model with the experimental results, the parameter called maximum adsorption layer or monolayer adsorption layer is observed. In addition to this, the K value found from the Langmuir model is a parameter related to adsorption and is considered as a measure of the adsorbent's affinity to the adsorbent. The Freundlich model is related to the heterogeneity of the adsorption surface, and the value in the range of 0–1 indicates that the adsorption of the lead ion by the fungus is favorable under the conditions studied.

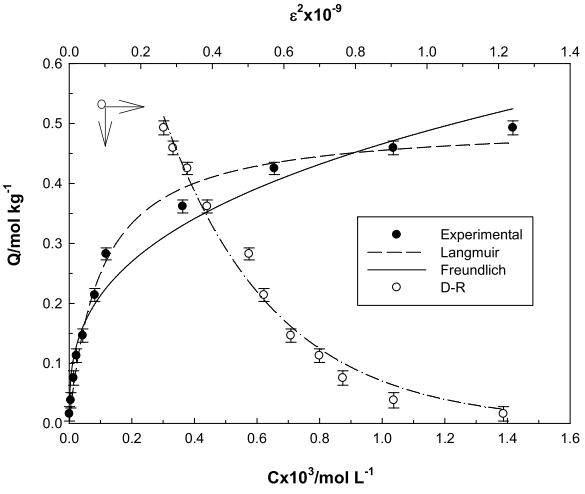

Fig. 2. The variation of Pb^{2+} concentration on biosorption by fungal biosorbent and its adaptation to Langmuir, Freundlich and D-R models ($[Pb^{2+}]_0$ = 10-600 mg L^{-1}, biosorbent dosage = 30 mg, V = 10 mL, pH = 4.0, contact time:24 h, temperature: 25 °C).

3.5. Biosorption kinetics

The biosorption kinetics of Pb^{2+} onto fungal biosorbent was presented in Table 2 and the graphs were given in Supplementary File 4. According to the Supplementary File 4, the adsorption is completed in about 4 h and reaches equilibrium. Therefore, 24 h was considered sufficient time for adsorption.

One of the factors affecting adsorption is the adsorption time. The transfer of the adsorbate to the adsorbent surface and the surface film formation, diffusion to surface pores, diffusion into the particle, and adsorption on the active centers on the pore surfaces determine the kinetics of the entire adsorption process. Some of these events are rapid, such as adsorption of active centers, but some events occur quite slowly and this is effective in determining the adsorption rate and the order of adsorption kinetics. The most widely used models for determining adsorption kinetics are Lagergren (pseudo-first-order, PFO), pseudo-second-order (PSO), and intraparticle diffusion (IPD) models. Since it is difficult to explain the kinetics of the adsorption process, in which more than one event takes place simultaneously or sequentially, with a single model, the adsorption kinetics are generally explained by its compatibility with more than one kinetic model. Although the coefficients of adaptation to real values, that is regression coefficients of the models, are mostly used in the evaluation of these models, the proximity of the adsorption value found when the adsorption reaches equilibrium and the adsorption value found from the model is considered as a reason for the use of the model in defining the adsorption kinetics.

While the PFO model only explains the adsorption kinetics in which desorption is neglected and has a high initial concentration and has little change in initial concentration or surface coating change, the PSO model is significant in adsorption with a lower initial concentration and reaction-controlled adsorption. The amount of adsorbate due to desorption does not change significantly during the adsorption period.

One of the other adsorption mechanisms that affect kinetics is diffusion into the particle. According to this model, the fact that the relevant graph passes through its origin and is multi-linear indicates that the diffusion rate into the particle also affects the adsorption kinetics. The adsorption chart presented in the study is multilinear, although it does not pass through its origin. This result shows that the adsorption kinetics of lead ions to the fungal biosorbent is one of the stages that determine the speed of diffusion into the particle in adsorption kinetics.

Correlation coefficients, which are a measurement of the fitness of biosorption to kinetic models, are used to determine the appropriate model. When the correlation coefficients of the PFO and PSO kinetic models were compared, it was seen that the biosorption kinetics were more suitable for the PSO kinetic model. Because when the experimentally calculated Q_t values the theoretically calculated Q_e values were examined (Table 2), it was seen that the PSO kinetic model results were closer to each other. In this case, it has shown that the biosorption process is better adapted to PSO kinetics. The PSO model predicts the rate of biosorption by mass transfer with low initial concentrations.

Table 1
Langmuir, Freundlich and Dubinin-Radushkevich isotherm models parameters.

Langmuir			Freundlich			Dubinin-Radushkevich			
X_L	K_L	R^2	K_f	β	R^2	X_{DR}	$-K_{DR}x10^9$	E_{DR}	R^2
0.501	4976	0.991	4.87	0.340	0.967	1.21	3.25	12.4	0.984

*X_L (mol kg^{-1}), K_L (L mol^{-1}), X_{DR} ($molkg^{-1}$), $-K_{DR}x10^9$ (mol^2KJ^{-2}), E_{DR} (kJ mol^{-1}).

Table 2
Parameters derived from adherence to pseudo-first-order, pseudo-second-order, and intraparticle diffusion kinetic models.

Kinetic models	Q_e/mol kg^{-1}	Q_t/mol kg^{-1}	$Hx10^3$/mol kg^{-1} min^{-1}	*(k_1, k_2, k_i) $x10^3$	R^2
PFO	0.412	0.481	14.7	35.8	0.881
PSO	0.459	0.481	34.1	92.6	0.930
IPD	–	–	–	237	0.948

* k_1: dk^{-1}, k_2: $mol^{-1}kgmin^{-1}$, k_i: $molkg^{-1}$ $min^{-0.5}$.

However, diffusion into the particle also plays an active role in the biosorption process. The IPD model assumes that diffusion is the decisive step to control the biosorption rate. In addition, IPD has two linear components; The adsorption process takes place primarily at active centers on the surface of the fungal biomass, and then diffusion into the pores of the fungal biomass occurs gradually.When the two models (PSO and IPD) are evaluated together, the kinetics of Pb^{2+} biosorption into fungal biomass can be explained by the rapid diffusion of the surface and the relatively slow diffusion of particles. A similar result to this situation has already been seen in the previous study about the Pb^{2+} adsorption on the lichen surface [27].

3.5.1. Mass transfer kinetics

3.5.1.1. Linear regression. MT is the transport of mass from the high to low concentration [29]. In this work, the mass transfer kinetics were modeled according to the MTF equations [30]. According to Supplementary File 5, a very good fit to the experimental data was verified by the graph of the straight line $R^2 > 0.946$, Table 3). Therefore, the use of the parameters B and β could be useful to describe the different kinetic mechanisms of Pb^{2+} ion biosorption onto fungal biosorbent. Biosorption of Pb^{2+} onto fungal biosorbent depends on the behavior of Pb^{2+} ions passing through three successive points of extracellular precipitation located outside of the biomass, cell surface biosorption located at interfacial water-biomass, and intracellular accumulation located within the biomass [31]. Therefore, the starting point for the analysis of the biosorption mechanisms involved in the transport of Pb^{2+} ions from the bulk solution to the surface of fungal biosorbent has been suggested to be dependent on GMT, EMT, and IMT [29].

3.5.1.2. Kinetics of GMT, EMT, and IMT. The determination of mass transfer resistance for the biosorption of Pb^{2+} ions onto fungal biosorbent is important in the analysis of the biosorption mechanisms [29]. Therefore, graphs of plotting $[k_La]$ versus the C_s/C_0 ratio can be used to predict the rates of GMT, EMT, and IMT. According to Supplementary File 6, the potential mass transfer as represented by the curve of $[k_La]_g$ is forceful at the beginning of depositing the Pb^{2+} ions and decreases exponentially with the increase of the solute accumulated onto the fungal biosorbent. This describes that the rate of mass transfer is still rapid for the amount of the Pb^{2+} ions accumulated onto fungal biosorbent. The attractive capability of the fungal biosorbent decreases with the increase of the Pb^{2+} ions accumulated. The resistance of mass transfer is therefore dependent on both the porous diffusion and film mass transfer. Because the attractive capability for the fungal biosorbent to adsorption Pb^{2+} ions in aqueous solution decreases with an increasing amount of the Pb^{2+} ions accumulated so the variations of $[k_La]_d$ or $[k_La]_f$ after passing an outflow decrease progressively.

Table 3
Values of β and B, obtained from plotting q versus ln(t).

C_0 (mg L^{-1})	B (kg mol^{-1} min)	B (mol kg^{-1})	R^2
300	0.0797	−0.021	0.946

3.6. Biosorption thermodynamics

The thermodynamic behavior of Pb^{2+} ions biosorption onto fungal biosorbent was studied at temperatures of 5 °C, 25 °C, and 40 °C. In Supplementary File 7 (ln K_D-1/ T) the values of ΔH° and ΔS° were calculated from the slope of the graph and the cut-off, respectively. Adsorption enthalpy was found positive. ΔH° was calculated as 32.1 kJ mol^{-1} indicated that the adsorption process was endothermic. ΔS° was calculated as 191 $Jmol^{-1}$ K^{-1}. The Gibbs free energy value was found as -21.1 kJ mol^{-1} at 25 °C. The negative Gibbs free energy value indicated the possibility of spontaneous adsorption.

Adsorption enthalpy was found positive. This shows that it is a heat consuming event during adsorption. The result is compatible with most metal adsorption studies. Adsorption entropy showed a positive increase in the disorder parameter. The entropy value found in adsorption from aqueous solution is not only applicable to the adsorption of the ion but also for the whole process. This positivity is due to the secondary interactions associated with adsorption, for example, dehydration, ion exchange, hydrolysis. Adsorption free enthalpy was found negative as expected. This result indicates that adsorption occurs spontaneously.

3.7. Biosorption-desorption performance

The re-use of biosorbent is very important to make the biosorption process cost-effective. Reusability of the desorption ability of Pb^{2+} ions onto fungal biosorbent was investigated. The fungal biosorbent was regenerated using HCl, NaOH, HNO_3, and ethyl alcohol, and the results were given in Fig. 3. The maximum recovery percentage for Pb^{2+} ions onto fungal biosorbent was achieved with HCl (61 %). The minimum recovery percentage for Pb^{2+} ions onto fungal biosorbent was achieved with ethyl alcohol (3.7 %).

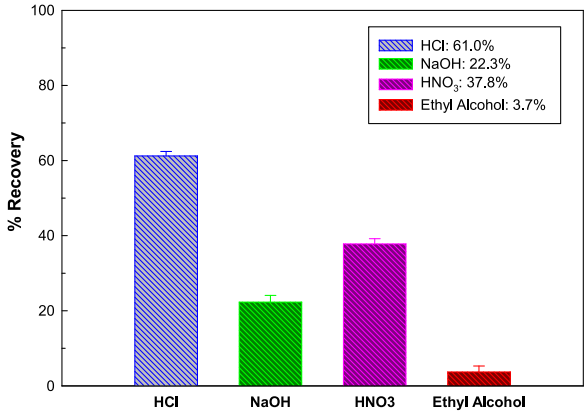

Fig. 3. The percentage of the recovery in various solvents for desorption of Pb^{2+} ions ($[Pb^{2+}]_0 = 300$ mg L^{-1}, biosorbent dosage = 30 mg, V = 10 mL, pH = 4.0, contact time:24 h, temperature: 25 °C).

3.8. Infrared spectroscopy coupled with pattern recognition techniques

Infrared spectra of samples (UL and PL groups) indicated obvious changes in both the fingerprint (1800−650 cm^{-1}) and CH (3000−2800 cm^{-1}) spectral regions (Supplementary File 8). However, the interaction of functional groups of fungal biosorbent with Pb^{2+} ions during the biosorption process was specifically determined by pattern recognition techniques developed on the big infrared spectral datasets, for better and reliable resolution of the prominent changes. The analyses ensured to identify the molecular modifications on the surface of unloaded (UL) and Pb^{2+} loaded (PL) fungal biosorbent.

PCA and HCA models which were developed on a dataset of fingerprint spectral region (1800−650 cm^{-1}) have been provided in Fig. 4 for UL and PL groups. As can be seen from the scores plot, the UL group was clustered as negative scores, however, the PL group was found as positive scores along the PC1 (49 %) (Fig. 4a). The loadings plot revealed 1 positive and 5 negative discriminators (Fig. 4b). Biologically, each of these discriminators represents the specific molecular modulation. In the interpretation of these modulations, we considered the link between scores (either negative or positive) and negative and/or positive discriminators. In other words, the scores (samples) values are bigger than the mean of all samples for a particular discriminator, provided that the signs (positive or negative) of scores and discriminator's loading value are identical on an examined PC. If these signs are opposite, the values of scores are lesser than the average values for a particular discriminator. The big values on both scores and loadings plots indicate a powerful correlation and vice-versa.

To interpret the correlated data, the negative discriminators at 1670 cm^{-1} (band 2) and 1600 cm^{-1} (band 3) represent the amide spectral region of proteins [34]. The other negative discriminators were assigned to various molecular alterations such as C═O vibrations of ester groups in triacylglycerols (band 1/ 1745 cm^{-1}), CH2 bending vibrations in lipids (band 4/ 1455 cm^{-1}), and C—O vibrations in polysaccharides (band 5/ 1105 cm^{-1}). The vibrational states of all these bands were negatively correlated with the scores of the PL group. In other words, these variables were found lower in the PL group compared with their average values, indicating the specific modulations in the represented biomolecules, as a result of Pb^{2+} loading. The positive discriminator at 966 cm^{-1} (band 6) assigned to C—C vibrational stretching of the DNA backbone [35] was found greater in the PL group concerning its average value (positive correlation), indicating alterations in DNA backbone. The PCA result was also confirmed by HCA ran on the same fingerprint region, as clear-cut discriminatory dendrogram was obtained between the UL and PL groups (Fig. 4c).

Fig. 5a and b represent scores and loadings plots of the PCA model, while the dendrogram of the HCA model is given in Fig. 5c in the CH region (3000−2800 cm^{-1}) for UL and PL groups. The CH region is generally considered to be associated with vibrational stretches in NH and CH functional groups of proteins and fatty acids, respectively [36–38]. According to the scores plot (Fig. 5a), the UL group was segregated in the negative side (negative scores), whereas the PL group was clustered in the positive side (positive scores) along the PC1. In all data analysis, we considered PC1 because it represents the largest (93 %) proportion of data standing behind the discrimination. A PC1 loadings

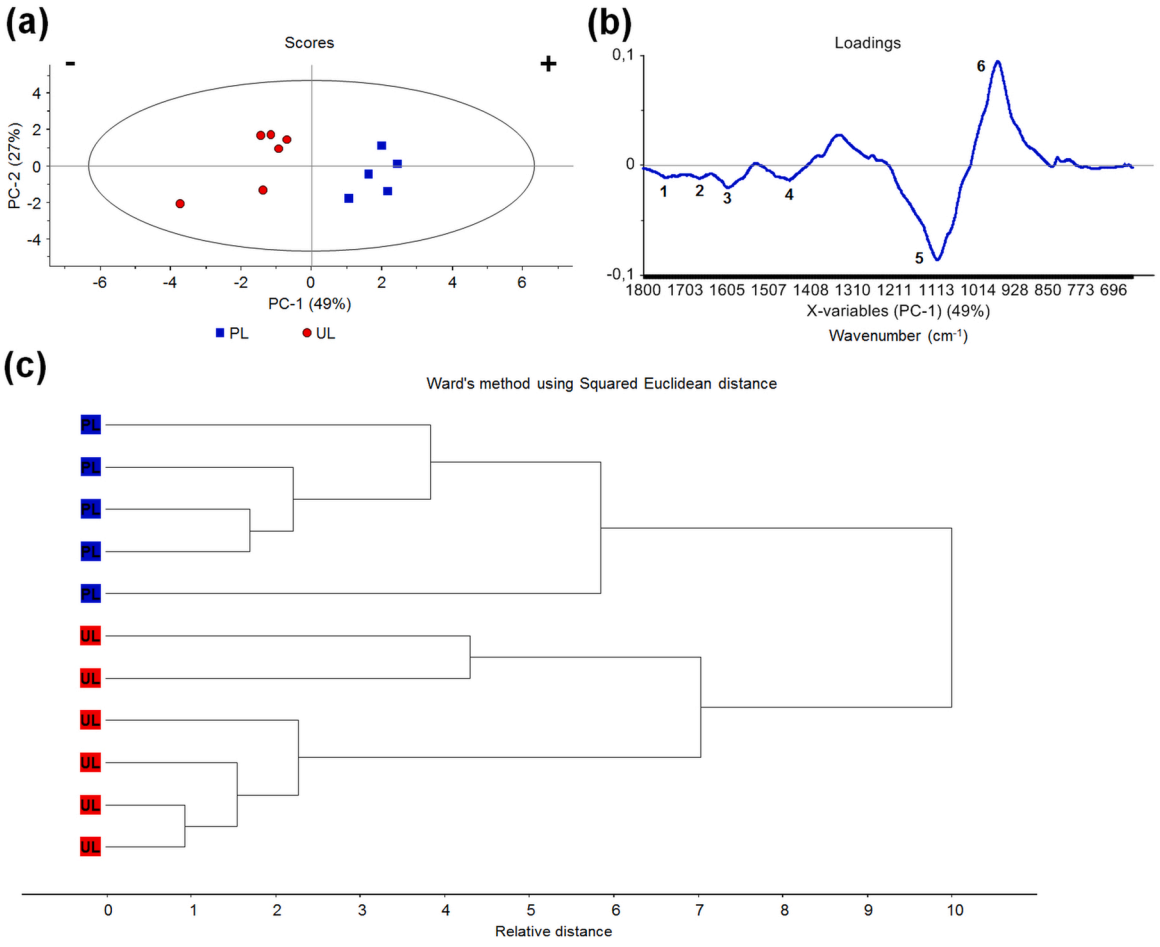

Fig. 4. Interaction of Pb2+ ions with functional groups of fungal biosorbent as revealed by pattern recognition techniques at fingerprint (1800-650 cm^{-1}) spectral region. (a) Scores plot and (b) Loadings plot of principal component analysis for UL and Pb groups. (c) The dendrogram of hierarchical cluster analysis for UL and Pb groups.

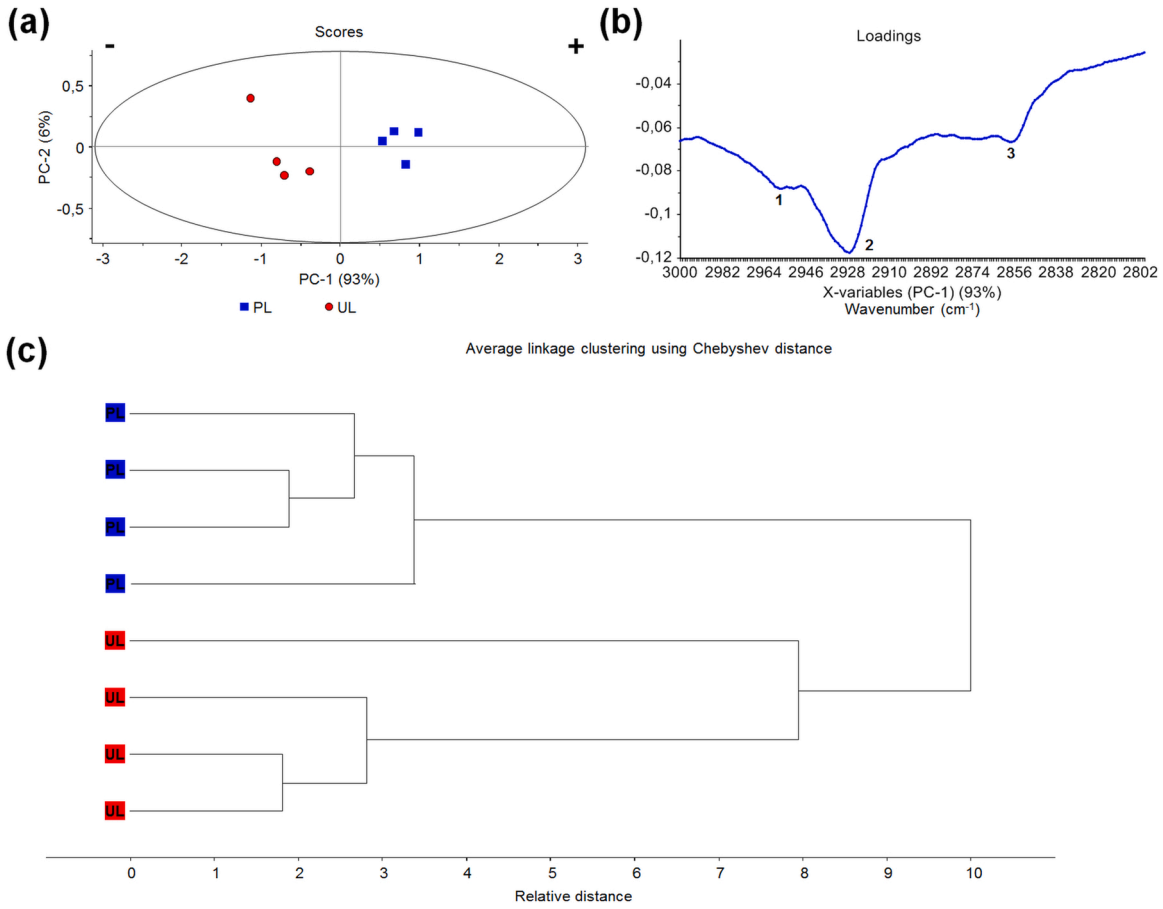

Fig. 5. Interaction of Pb^{2+} ions with functional groups of fungal biosorbent as revealed by pattern recognition techniques at CH (3000-2800 cm^{-1}) spectral region. (a) Scores plot and (b) Loadings plot of principal component analysis for UL and PL groups. (c) The dendrogram of hierarchical cluster analysis for UL and Pb groups.

plot indicates that the discrimination seen in the scores plot emerges from variations in negative discriminators (bands 1, 2, and 3) (Fig. 5b). The negative discriminators at 2958 cm^{-1} (band 1), 2928 cm^{-1} (band 2), and 2858 cm^{-1} (band 3) correspond to vibrational stretching of CH groups in acyl chains of fatty acids [34; 37]. The UL group was found as negative scores (same sign with discriminators of loadings plot), however, the correlation of scores and loadings plots demonstrate the opposite signs between the PL group (positive) and discriminators on the loadings plot (negative). Therefore, the correlated data mean that vibrational stretches of CH of acyl chains in the PL group are less than their corresponding average values. In other words, Pb^{2+} loading led to changes in fatty acid molecules. The distinct discrimination in the dendrogram obtained by HCA in the CH region was also supportive (Fig. 5c). The results of both PCA and HCA models obtained for the CH region are complementary with the results obtained in the fingerprint region (Fig. 4).

The results indicated that the surface of the fungal biosorbent prepared from *R. arrhizus* biomass has diverse functional groups interacting with metal ions (Figs. 4 and 5). It was known that the major site for metal biosorption on the fungal surface was the fungal wall [21]. Feofilova, 2010 reported that the composition of the fungal cell wall was dominantly polysaccharides (80 %) and also proteins (3–20 %) [39]. The analyses of the fungal biosorbent revealed the characteristic spectral bands originating from divergent functional groups of biological molecules interacting with Pb^{2+} ions. Presumably, the changes in the stretching of various functional groups are associated with the interaction of Pb^{2+} ions with active sites of fungal biosorbent. Previous studies showed that electrostatic interactions are important in the chemical attraction of Pb^{2+} ions by active sites of fungal biosorbent [40, 41].

3.9. SEM analysis

The surface morphology and bulk structure of the unloaded and metal ion loaded fungal biosorbent was investigated by the scanning electron micrographs and were given in Fig. 6. The scanning electron micrograph showing the sporangium of *R. arrhizus* composed with a mass of spores of the fungus (Fig. 6a). The surface morphology of the fungal sample (Fig. 6a) was conspicuously different from that of the metal loaded one (Fig. 6b). The smooth surface of the sporangium and mycelia of the fungus (Fig. 6c), turned rough and irregular after the biosorption of metal ions (Fig. 6d). Highly magnified images showed that the surface of unloaded samples (Fig. 6e) was rigid but the surface of metal loaded samples (Fig. 6f) was roughly indicating the adsorption of Pb^{2+} ions on the sporangium surface.

Fig. 7a and 7b show the EDX spectra before/after Pb^{2+} biosorption onto fungal biosorbent. According to the results in Fig. 7a, the fungal biosorbent contained elements C, O, Ca, Cl, and K. On the other hand, the presence of Pb^{2+} ions, as well as all elements of the fungal biosorbent in Figure 7b, was the evidence for Pb^{2+} biosorption onto the fungal biosorbent. The results of EDX mapping analysis also supported the Pb^{2+} biosorption onto the surface of fungal biosorbent (Supplementary File 9). The biosorption process involves different mechanisms for binding metal ions. These can be divided into metabolism-dependent and metabolism-independent processes according to the dependence of the biosorption mechanism on cell metabolism. According to the location where metal ions are removed from the solution, the biosorption process can be classified as i) cell-surface biosorption ii) intracellular accumulation and iii) precipitation/extracellular accumulation. Biosorption of metal ions to the cell surface occurs between functional groups on the

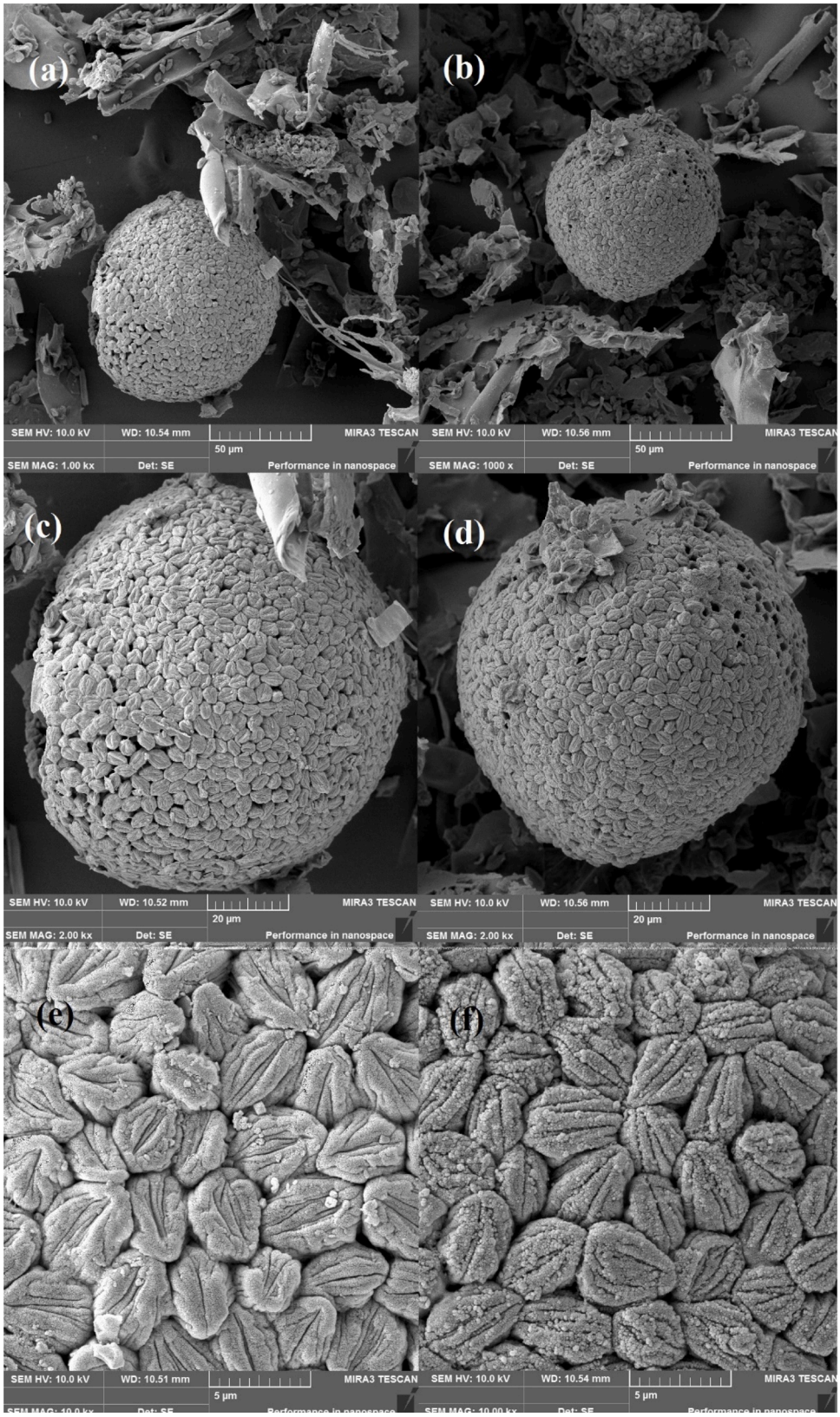

Fig. 6. SEM photographs of fungal biosorbent before (a, c, e) and after (b, d, f) biosorption of Pb^{2+} ($[Pb^{2+}]_0 = 300$ mg L^{-1}, biosorbent dosage = 30 mg, V = 10 mL, pH = 4.0, contact time:24 h, temperature: 25 ◦C).

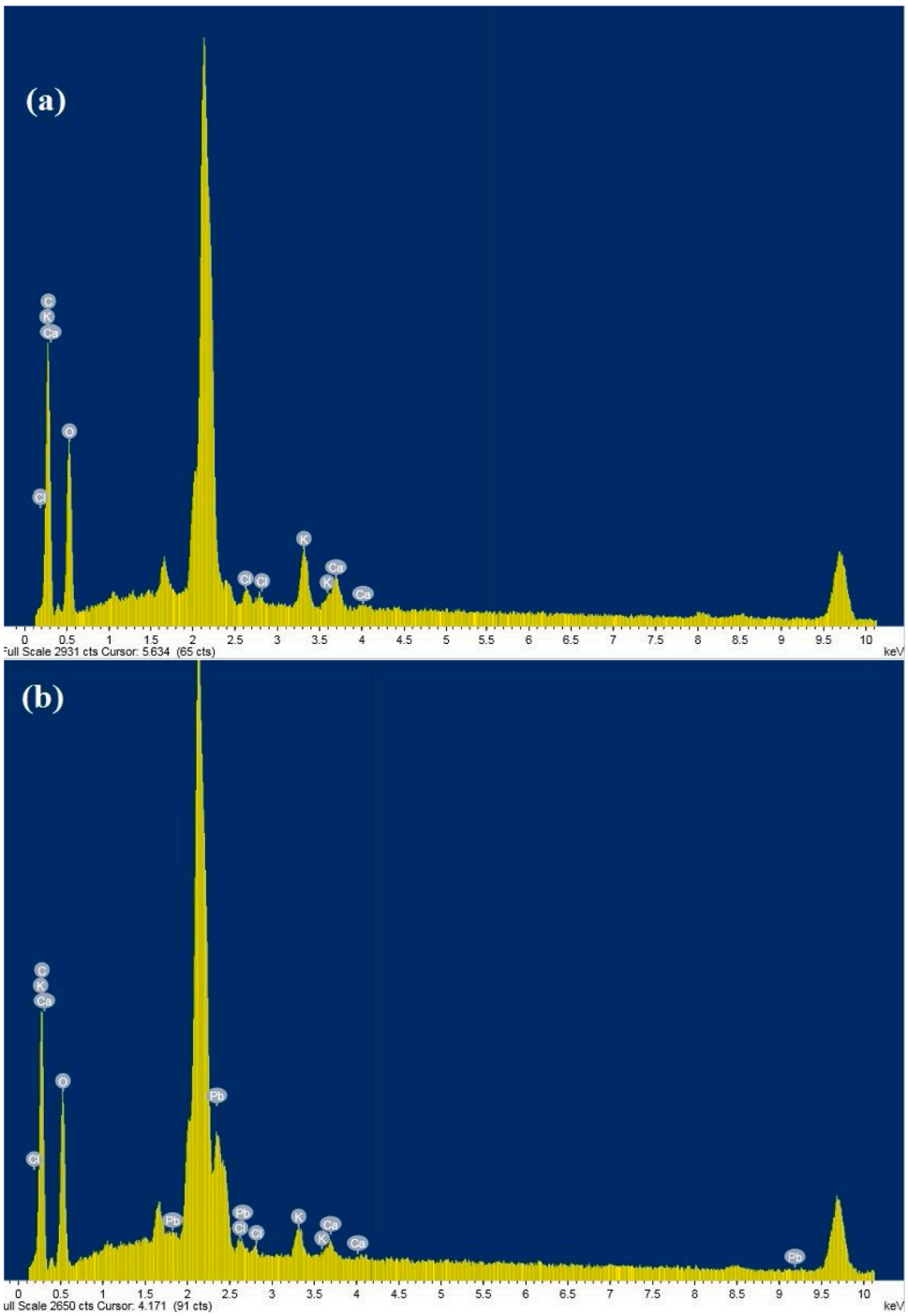

Fig. 7. EDX spectrum of fungal biosorbent before (a) and after (b) biosorption of Pb^{2+}. ($[Pb^{2+}]_0 = 300$ mg L^{-1}, biosorbent dosage = 30 mg, V = 10 mL, pH = 4.0, contact time:24 h, temperature: 25 ◦C).

cell surface and metal ions, and this is based on physical biosorption. This type of biosorption is not dependent on metabolism, it is relatively fast and reversible. Intracellular accumulation occurs only in living cells. In the case of precipitation/extracellular accumulation, the biosorption process can occur both in solution and at the cell surface. Each of these three mechanisms is a process that occurs independently, and the biosorption process is considered to be a combination of several of these mechanisms [42].

According to the results of this study, the binding mechanism of Pb^{2+} ions to the fungal biosorbent involves at least a two-step process. The first step is the interaction between Pb^{2+} ions with functional groups in the cell wall (glucans, polysaccharides, mannoproteins, and chitin). The second stage is the inorganic accumulation of Pb^{2+} ions. FT-IR analysis results also revealed characteristic spectral bands originating from functional groups of fungal biosorbent interacting with Pb^{2+} ions. Changes in the stretching of functional groups of fungal biosorbent after Pb^{2+} biosorption are related to the interaction of Pb^{2+} ions with active centers in functional groups in the fungal biosorbent. Besides, changes in SEM images after Pb^{2+} biosorption and EDX analysis results also support Pb^{2+} biosorption into active centers in the fungal biosorbent.

The reported studies about the metal biosorption properties of the genus *Rhizopus* were presented in Table 4. According to Table 4, Sağ et al. (2000) showed that the Pb^{2+} ion biosorption capacity of *R. arrhizus* was 12.31 mg g^{-1} with a 200 mL working solution including 20 mL

Table 4
The comparison of heavy metal removal capacity of fungal species belonging to the *Rhizopus* genus (Hm: heavy metal; C_o: Initial metal concentration; T: Temperature; Bd: Biosorbent dosage; Ar: Agitation rate; Q_m: Adsorbed capacity).

Fungal species	Hm	C_o	pH	T (°C)	Bd	Ar (rpm)	Q_m (mg g^{-1})	Refs.
R. arrhizus	Cd^{2+}	50 mg dm^{-3}	3.5	30	20 mL	150	11.17	[19]
R. arrhizus	Pb^{2+}	50 mg dm^{-3}	4	25	20 mL	150	12.31	[19]
R. arrhizus	Cu^{2+}	50 mg dm^{-3}	4.5	30	20 mL	150	7.32	[19]
R. arrhizus	Pb^{2+}	2.80 mg L^{-1}	4.5	30	1 g L^{-1}	120	2.64	[20]
R. oryzae	Pb^{2+}	200 mg L^{-1}	4	25	2 g L^{-1}	100	69.73	[21]
R. oryzae	Co^{2+}	200 mg L^{-1}	7	25	2 g L^{-1}	100	13.56	[21]
R. oligosporus	Pb^{2+}	200 mg L^{-1}	5	30	0.5 g L^{-1}	200	126.00	[17]
R. arrhizus	Pb^{2+}	200 mg L^{-1}	5	25	1 g L^{-1}	150	50.42	[18]
R. arrhizus	Cu^{2+}	200 mg L^{-1}	4	25	1 g L^{-1}	150	31.23	[18]
R. arrhizus	Pb^{2+}	300 mg L^{-1}	4	25	3 g L^{-1}	150	103.70	This Study

fungal suspension dosage at pH 4 and 25 °C [18]. In the current work, the optimal biosorbent dosage was found 3 mg g^{-1}, which was higher than Sağ et al. (2000) used [18]. Although other parameters such as pH, agitation rate, and temperature were the same, biosorbent dosage was different and the biosorption capacity was found higher in the current work. Besides, the results of the current work showed that the biosorption rate was diminished by decreasing the biosorbent dosage. Similarly, Uslu et al. (2003) studied the Pb^{2+} removal rate of *R. arrhizus* and reported that the fungus performed 50.42 mg g^{-1} Pb^{2+} biosorption capacity at 200 mg L^{-1} Pb^{2+} ion concentration and 25 °C with 1 g L^{-1} biosorbent dosage [19]. Although the biosorbent dosage, agitation rate, and temperature were the same as the current work, the initial Pb^{2+} ion concentration was lower than the results of the current study. The optimal ion concentration was determined as 300 mg L^{-1} and it has also been proven that the biosorption capacity was enhanced by increasing the initial Pb^{2+} concentration. Among the heavy metal biosorption capacity of the fungal species reported by the previous studies, the *R. arrhizus* fungus used in this study performed the most successful Pb^{2+} removal capacity from aqueous solutions under the determined optimal conditions.

The results of this study also show that the total amount of biosorbent removes 103.70 mg of Pb^{2+} ions per gram. This efficient metal removal was carried out at room temperature using 3 g of biosorbent per liter. Approximately 500 mL of molasses medium was used to obtain 1 g of dried biosorbent during the study. The molasses medium contained molasses provided free of charge from the factory as a carbon source, and relatively inexpensive ammonium sulfate as a nitrogen source for microbial growth [43]. In this case, it reduces the cost of the whole process. Besides, the use of room temperature also reduces the production and especially energy costs in large-scale fermenters. In light of this information, this study optimized the mycosorption of Pb^{2+} by *R. arrhizus* and revealed the optimal conditions to obtain the best removal performance. Many studies previously published in the literature support the view that fungal biomass can be an economical biosorbent [6–8,17–21,31,41,42,44]. Some studies have even shown that the fungal biomass used in production for different purposes is an economical and cheap biosorbent [44]. It has also been reported in the literature that *R. arrhizus*, the fungus used in this study, can be used in the production of lactic acid, which is an important biotechnological product [45]. In another study conducted in recent years, it has been reported that *R. arrhizus* can be used successfully in the commercial production of Fumaric acid, a biotechnological product [46]. In this context, it is thought that the waste *R. arrhizus* biomass generated as a result of the production of other commercial products can be used as a cheap and efficient biosorbent as shown in this study.

The detailed examination of Table 4 revealed that both Pb^{2+} and other metals such as Cu^{2+} and/or Cd^{2+} removals of *R. arrhizus* species were already investigated. For example, Uslu et al. (2003) studied the optimization of *R. arrhizus*'s Cd^{2+}, Pb^{2+}, and Cu^{2+} removals, and showed that this fungus achieved the best Pb^{2+} removal among others [19]. Also, Sağ et al. (2000) [18] examined the biosorption of Pb^{2+} and Cu^{2+} by the *R. arrhizus* and achieved higher removal capacity than Uslu et al. (2003) [19] showed. In this case, the literature supports the possibility of obtaining different results because of the change of optimal conditions and this current study was conducted due to the necessity of re-examination of this situation. Besides, both Sağ et al. (2000) [18], as well as Uslu et al. (2003) [19], showed that the fungus performed the best Pb^{2+} removal compared to other metals, which indicates that the fungus has a greater affinity for Pb^{2+}. Therefore, only Pb^{2+} was investigated as a metal in this study. In this study, the parameters for Pb^{2+} removal were kept in a wide range and the optimal conditions were tried to be determined clearly. On the other hand, the previous studies reported that the fungus can successfully remove metals such as Cu^{2+} and Cd^{2+}, albeit less than Pb^{2+} (Table 4).

This study determined that there is a chemical interaction between the fungal surface and Pb^{2+} ions in the mycosorption mechanism. In this case, the mycosorption mechanism of Pb^{2+} prevails other metals such as Cu^{2+}, Cd^{2+}, which have similar chemical properties with Pb^{2+}.

4. Conclusions

This study aims to optimize the Pb^{2+} removal potential of fungal biomass obtained from *R. arrhizus* and also to explain the mechanism of mycosorption. The optimal conditions for maximum removal capacity were pH 4, 25 °C, and 150 rpm agitation rate with 300 mg L^{-1} initial ion concentration and 3 g L^{-1} biosorbent dosage. The maximum mycosorption capacity was found 103.70 mg g^{-1} at the determined optimal conditions. Under optimal conditions, the monolayer adsorption capacity was calculated as 0.501 mol kg^{-1} from the Langmuir isotherm model. The biosorption free energy was found to be EDR (16.2 kJ mol^{-1}), showing that the adsorption proceeds chemically. The biosorption kinetic of Pb^{2+}ions onto fungal biosorbent was suitable with the PSO kinetic model. The use of the MTF models to simulate the experimental data was able to provide a more complete understanding of the biosorption kinetic mechanisms of Pb^{2+} ions onto fungal biosorbent. The resistance of mass transfer for the biosorption of Pb^{2+} ions onto fungal biosorbent from aqueous solution may be mainly dependent on EMT. Thermodynamic parameters showed that Pb^{2+} biosorption by the fungus was spontaneous and endothermic. The results of the characterization analysis supported that the compounds forming the structure of the fungal cell wall and its chemical structure allow metal ions such as Pb^{2+} to be chemically adsorbed. On the other hand, it was revealed that the desorption of Pb^{2+} ions is maximally achieved in acidic conditions. According to the results of this study, the most important factor for *R. arrhizus* being a successful biosorbent in heavy metal removal is the chemical structure of the cell wall.

To sum up, fungal biosorbent has very good properties such as high biosorption capacity for lead ions, easy and economic preparation, environmentally friendly, thermodynamically favorable, high biosorption, effective, and cheap biosorbent, compatible with the green chemistry concepts.

CRediT authorship contribution statement

Zeynep Mine Şenol: Investigation, Validation, Visualization. **Ülküye Dudu Gül:** Supervision, Conceptualization, Writing - original draft, Writing - review & editing. **Rafig Gurbanov:** Formal analysis, Writing - review & editing. **Selçuk Şimşek:** Resources, Writing - review & editing.

Declaration of Competing Interest

The authors report no declarations of interest.

Acknowledgment

The present study was partly supported by the Cumhuriyet University Scientific Research Projects Commission (Project NO: ZARA-005), Sivas, TURKEY.

Appendix A. Supplementary data

Supplementary material related to this article can be found, in the online version, at doi:https://doi.org/10.1016/j.jece.2020.104760.

References

[1] N. Saeidi, M. Parvini, Z. Niavarani, High surface area and mesoporous graphene/activated carbon composite for adsorption of Pb(II) from wastewater, J. Environ. Chem. Eng. 3 (2015) 2697–2706, https://doi.org/10.1016/j.jece.2015.09.023.
[2] J. Marta, A. Rorat, A. Grobelak, Enzymatic assays confirm the toxicity reduction after manure treatment of heavy metals contaminated soil, S. Afr. J. Bot. 124 (2019) 47–53, https://doi.org/10.1016/j.sajb.2019.04.035.
[3] T. Amari, T. Ghnaya, C. Abdelly, Nickel, cadmium, and lead phytotoxicity and potential of halophytic plants in heavy metal extraction, S. Afr. J. Bot. 111 (2017) 99–110, https://doi.org/10.1016/j.sajb.2017.03.011.
[4] M. Taghi Ganji, M. Khosravi, R. Rakhshaee, Biosorption of Pb, Cd, Cu and Zn from the wastewater by treated *Azolla filiculoides* with H2O2/MgCl2, Int. J. Environ. Sci. Technol. (Tehran) 1 (2005) 265–271, https://doi.org/10.1007/BF03325841.
[5] Ü.D. Gül, B.E. Taştan, G. Bayazıt, Assessment of algal biomasses having different cell structures for biosorption properties of acid red P-2BX dye, S. Afr. J. Bot. 127 (2019) 147–152, https://doi.org/10.1016/j.sajb.2019.08.047.
[6] Ü.D. Gül, Treatment of dyeing wastewater including reactive dyes reactive red RB reactive black B remazol blue and methylene blue by fungal biomass, Water SA 39 (2013) 593–598.
[7] J.D. He, Y.D. Wang, N. Hu, D. Ding, J. Sun, Q.W. Deng, C.W. Li, F. Xu, An artificially constructed Syngonium podophyllum- *Aspergillus niger* combinate system for removal of uranium from wastewater, Environ. Sci. Pollut. Res. 22 (2015) 18918–18926.
[8] E. Azin, H. Moghimi, Efficient mycosorption of anionic azo dyes by *Mucor circinelloides*: surface functional groups and removal mechanism study, J. Environ. Chem. Eng. 6 (2018) 4114–4123, https://doi.org/10.1016/j.jece.2018.06.002.
[9] R. Garcia-Rubio, H.C. de Oliveira, J. Rivera, N. Trevijano-Contador, The fungal cell wall: candida, Cryptococcus, and Aspergillus species, Front. Microbiol. 10 (2020) 2993, https://doi.org/10.3389/fmicb.2019.02993.
[10] N.A.R. Gow, J.-P. Latge, C.A. Munro, The fungal cell wall: structure, biosynthesis, and function, Microbiol. Spectrum 5 (2017) 1–25, https://doi.org/10.1128/microbiolspec.
[11] A. Beauvais, J.-P. Latge, Fungal cell wall, J. Fungi Basel (Basel) 91 (2018) 1–8, https://doi.org/10.3390/jof4030091.
[12] J. Ruiz-Herrera, Fungal Cell Walls: Structure, Synthesis, and Assembly, CRC Press Inc., Boca Raton, Florida, 1992.
[13] L. Muszkieta, V. Aimanianda, E. Mellado, S. Gribaldo, L. Alcàzar-Fuoli, E. Szewczyk, M.-C. Prevost, J.-P. Latge, Deciphering the role of the chitin synthase families 1 and 2 in the in vivo and in vitro growth of *Aspergillus fumigatus* by multiple gene targeting deletion, Cell. Microbiol. 16 (2014) 1784–1805, https://doi.org/10.1111/cmi.12326.
[14] F.M. Klis, P. Mol, K. Hellingwerf, S. Brul, Dynamics of cell wall structure in *Saccharomyces cerevisiae*, FEMS Microbiol. Rev. 26 (2002) 239–256.
[15] R. Zarnowski, W.M. Westler, G.A. Lacmbouh, J.M. Marita, J.R. Bothe, J. Bernhardt, A. Lounes-Hadj Sahraoui, J. Fontaine, H. Sanchez, R.D. Hatfield, et al., Novel entries in a fungal biofilm matrix encyclopedia, MBio 5 (2014) e01333–14.
[16] N. Ali, A. Khan, S. Malik, S. Badshah, M. Bilal, H.M.N. Iqbal, Chitosan-based green sorbent material for cations removal from an aqueous environment, J. Environ. Chem. Eng. 8 (2020), 104064.
[17] A.B. Ariff, M. Mel, M.A. Hasan, M.I.A. Karim, The kinetics and mechanism of lead (II) biosorption by powderized *Rhizopus oligosporus*, World J. Microb. Biot. 15 (1999) 291–298.
[18] Y. Sağ, A. Kaya, T. Kutsal, Biosorption of lead(II), nickel(II), and copper(II) on *rhizopus arrhizus* from binary and ternary metal mixtures, Sep. Sci. Technol. 16 (2000) 2601–2617.
[19] G. Uslu, A.Y. Dursun, H.I. Ekiz, Z. Aksu, The effect of Cd(II), Pb(II) and Cu(II) ions on the growth and bioaccumulation properties of Rhiz*opus arrhizus*, Process Biochem. 39 (2003) 105–110.
[20] T. Bahadir, G. Bakan, L. Altas, H. Buyukgungor, The investigation of lead removal by biosorption: an application at storage battery industry wastewaters, Enzyme Microb. Technol. 41 (2007) 98–102.
[21] M.M. Gharieb, A.A. Al-Fakih, M.I. Ali, Biosorption of Pb(II) and Co(II) ions from aqueous solutions using pretreated *rhizopus oryzae* (Bread mold), Arab. J. Sci. Eng. 39 (2014) 2435–2446.
[22] R. Gurbanov, S.N. Ozek, S. Tunçer, F. Severcan, A.G. Gozen, Aspects of silver tolerance in bacteria: infrared spectral changes and epigenetic clues, J. Biophotonics 11 (5) (2018) e201700252, https://doi.org/10.1002/jbio.201700252.
[23] R. Gurbanov, H. Karadağ, S. Karaçam, G. Samgane, Tapioca starch modulates cellular events in oral probiotic *Streptococcus salivarius* strains, Probiotics & Antimicro. Prot. (2020), https://doi.org/10.1007/s12602-020-09678-z.
[24] P. Gemperline, Practical Guide To Chemometrics, second ed., CRC Press, Boca Raton, 2006.
[25] M.G. Miljkovic, S.Z. Davidovic, M.B. Carevic, D.N. Veljovic, D.D. Mladenovic, M. D. RajilicStojanovic, S.I. Dimitrijevic-Brankovic, Sugar beet pulp as *Leuconostoc mesenteroides* T3 for enhanced dextransucrase production on molasses, Appl. Biochem. Biotechnol. 180 (2016) 1016–1027.
[26] Y. Xie, H. Zhou, C. Liu, J. Zhang, N. Li, Z. Zhao, G. Sun, Y. Zhong, A molasses habitat-derived fungus *Aspergillus tubingensis* XG21 with high β-fructofuranosidase activity and its potential use for fructooligosaccharides production, AMB Expr. 7 (2017) 128.
[27] Z.M. Şenol, Ü.D. Gül, S. Şimşek, Assessment of Pb2+ removal capacity of lichen (*Evernia prunastri*): application of adsorption kinetic, isotherm models, and thermodynamics, Environ. Sci. Pollut. Res. (2019) 1–12, https://doi.org/10.1007/s11356-019-05848.
[28] M.A. Fulazzaky, Determining the resistance of mass transfer for adsorption of the surfactant onto granular activated carbons from hydrodynamic column, Chem. Eng. J. 166 (2011) 832–840.
[29] M.A. Fulazzaky, Analysis of global and sequential mass transfers for the adsorption of atrazine and simazine onto granular activated carbons from hydrodynamic column, Anal. Methods 4 (2012) 2396–2403.
[30] V. Javanbakht, H. Zilouei, K. Karimi, Lead biosorption by different morphologies of fungus *Mucor indicus*, Int. Biodeter. Biodegr. 65 (2011) 294–300.
[31] P. Velmurugan, J. Shim, Y. Yo, S. Choi, S. Kamala-Kannan, K.J. Lee, H.M. Kim, B. T. Oh, Removal of zinc by live, dead, and dried biomass of *Fusarium* spp. Isolated from the abandoned-metal mine in South Korea and its perspective of producing nanocrystals, J. Hazard. Mater. 182 (2010) 317–324.
[32] T. Manzoor, A. Shoaib, R. Bajwan, Mycoremediation of Cu(II) and Ni(II), Afr. J. Microbiol. Res. 6 (2012) 236–244.
[33] Z. Kiliç, O. Atakol, S. Aras, D. Cansaran-Duman, E. Emregul, Biosorption properties of zinc(II) from aqueous solutions by *Pseudevernia furfuracea* (L.) Zopf, J. Air Waste Manage. 64 (2014) 1112–1121.
[34] Z. Movasaghi, S. Rehman, I. Ur Rehman, fourier transform infrared (FTIR) spectroscopy of biological tissues, Appl. Spectrosc. Rev. 43 (2008) 134–179, https://doi.org/10.1080/05704920701829043.
[35] D. Naumann, D. Helm, C. Schultz, Characterization and identification of micro-organisms by FT-IR spectroscopy and FT-IR microscopy, in: F.G. Priest, A. Ramos-Cormenzana, B.J. Tindall (Eds.), Bacterial Diversity and Systematics. Federation of European Microbiological Societies Symposium Series, 75, Springer, Boston, MA, 1994, https://doi.org/10.1007/978-1-4615-1869-3_4.
[36] P. Lasch, D. Naumann, Infrared spectroscopy in microbiology. Encyclopedia of Analytical Chemistry, John Wiley & Sons, Ltd., 2015, https://doi.org/10.1002/9780470027318.a0117.pub2.
[37] C. Quintelas, E.C. Ferreira, J.A. Lopes, C. Sousa, An overview of the evolution of infrared spectroscopy applied to bacterial typing, Biotechnol. J. 13 (2018), https://doi.org/10.1002/biot.201700449.
[38] S. Garip, F. Bozoglu, F. Severcan, Differentiation of mesophilic and thermophilic Bacteria with fourier transform infrared spectroscopy, Appl. Spectrosc. 61 (2007) 186–192.
[39] E.P. Feofilova, The fungal cell wall: modern concepts of its composition and biological function, Microbiology 79 (2010) 711.
[40] I. Michalak, K. Chojnacka, A. WItek-KrowIak, State of the Art for the biosorption process- a review, Appl. Biochem. Biotechnol. 170 (2013) 1389.
[41] N.A. Salvi, Biosorption of Azo dyes by spent *Rhizopus arrhizuss* biomass, Appl. Water Sci. 7 (2017) 3041.
[42] R. Dhankhar, A. Hooda, Fungal biosorption–an alternative to meet the challenges of heavy metal pollution in aqueous solutions, Environ. Technol. 32 (2011) 467–491.
[43] V.R.O. Lopes, M.A. Farias, I.M.P. Belo, M.A.Z. Coelho, Nitrogen sources on tpomw valorization through solid state fermentation performed by *yarrowia lipolytica*, Braz. J. Chem. Eng. 33 (2016) 261–270.

[44] A.J. Legorreta-Castaneda, C.A. Lucho-Constantino, R.I. Beltran-Hernandez, C. Coronel-Olivares, G.A. Vazquez-Rodriguez, Biosorption of water pollutants by fungal pellets, Water 12 (2020) 1–38.

[45] B. Jin, L.P. Huang, P. Lant, *Rhizopus arrhizus*–a producer for simultaneous saccharification and fermentation of starch waste materials to L(+)-lactic acid, Biotechnol. Lett. 25 (2003) 1983–1987.

[46] A. Papadaki, M. N.Androutsopoulos, M. Patsalou, N. Koutinas, A.M. Kopsahelis, S. de Castro, A.A. Papanikolaou, Koutinas. Biotechnological production of fumaric acid: the effect of morphology of *rhizopus arrhizus* NRRL 2582, Fermentation 33 (2017) 1–13.